

# A Guide to the Application of Microperforated Panel Absorbers

David W. Herrin, Weiyun Liu, Xin Hua, and Jinghao Liu, University of Kentucky, Lexington, Kentucky

Microperforated panel absorbers are increasing in use because they are rugged, cleanable and aesthetically pleasing. Nevertheless, it is more difficult to integrate them into a design than the more commonly used fibers and foams. This is due to the fact that the microperforated panel absorber is best considered as a system, including the panel and the environment in which it is placed. Microperforated panels (MPPs) should be positioned carefully. Moreover, the backing cavity behind the MPP should be subdivided to improve the performance, and designed backings can further augment the performance. There are also practical issues. For example, there is some concern about the MPP becoming clogged with dust or other contaminants and becoming ineffective. Moreover, there are several types of MPP panels commercially available, but their property differences are not very well understood. This article is an attempt to deal with these questions and others that noise and vibration practitioners have.

Microperforated panel (MPP) absorbers have attracted a good amount of attention over the past two decades. An MPP is typically a metal or plastic panel with sub-millimeter-size holes or slits. The small perforation size differentiates them from traditional perforated panels, where perforations are normally several millimeters in size. The MPP functions by absorbing sound primarily due to high acoustic resistance in the perforate. So they are most effective when the particle velocity is high in the perforation.

At this time, they are primarily a niche absorber due to the low cost and effectiveness of traditional sound-absorbing materials like fibers and foams. Though inexpensive, fibers and foams cannot be used in many applications. They are easily damaged and have a relatively short lifespan in demanding environments. They are flammable when they soak up oils or other contaminants, and are difficult to clean or sterilize. High temperature and flow make traditional absorbers difficult to integrate into mufflers and silencers.

With that in mind, MPP absorbers are appealing despite the higher cost for performance reasons. Moreover, they are aesthetically pleasing and relatively lightweight. First-generation MPPs were made from metal and had circular laser-cut holes. Second-generation MPPs are less expensive because they are manufactured by etching, cutting, shearing, or grinding. They are now being used in a number of industrial, transportation, and architectural applications. Figure 1 shows a sample of a first-generation MPP along with one of the micro-slit variety (second generation).

MPP absorbers should be carefully integrated into a design. Incorporating fibers and foams is comparatively easier because they are effective at mid to high frequencies irrespective of their placement. So engineers can position them with little thought, and they are often added after a prototype has been made. The effectiveness of MPP absorbers, on the other hand, is normally compromised when they are added on an *ad hoc* basis.

A prior article in these pages<sup>1</sup> discussed applications and measurement procedures. Part of that information is repeated here for completeness. The focus of this article is on the integration of MPP absorbers into a design. It is particularly aimed at engineers who are considering implementing MPP absorbers into their products. In the course of the article, many common concerns will be addressed, such as the effect of dirt contamination and frequency tuning.

## Determining Properties

Porous absorber properties are normally determined using an impedance tube via ASTM E1050,<sup>2</sup> though they can also be determined to reasonable accuracy by measuring the flow resistivity via ASTM C522<sup>3</sup> and using an appropriate empirical equation.<sup>4</sup> The property of greatest interest is the sound absorption coefficient,

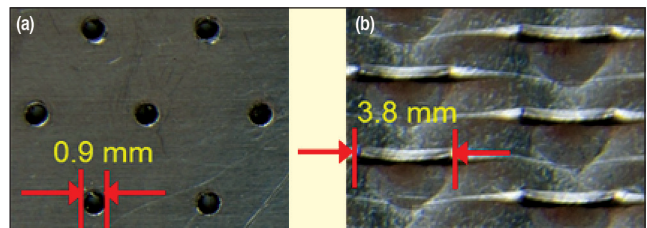


Figure 1. Schematic showing a MPP with (a) circular and (b) micro-slit perforations.<sup>1</sup>

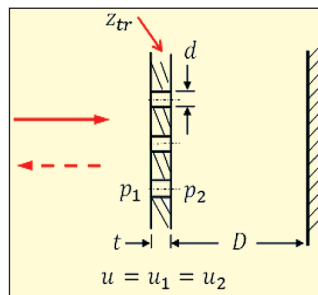


Figure 2. Schematic showing variables used in Maa's equation.<sup>1</sup>

which can be directly used in room acoustics equations or statistical energy analysis models. If needed, the normal incident impedance or bulk properties are also measured and can be used in numerical simulation (finite- or boundary-element models).

MPP absorber properties are straightforward to measure but are not so simple to interpret and use. The acoustic transfer impedance is normally used to

characterize an MPP. It is defined as:

$$z_{tr} = \frac{p_1 - p_2}{u} \quad (1)$$

where  $p_1$  and  $p_2$  are the measured sound pressures on either side of the panel, and  $u$  is the particle velocity. The variables are defined in Figure 2. The procedure for measuring the transfer impedance in an impedance tube using a simple impedance difference approach has been detailed previously.<sup>1</sup>

The transfer impedance can also be predicted using the well-known equation developed by Maa:<sup>5</sup>

$$z_{tr} = \frac{32\eta t}{\sigma d^2} \left( \left( 1 + \frac{\beta^2}{32} \right)^{\frac{1}{2}} + \frac{\sqrt{2}}{8} \beta \frac{d}{t} \right) + j \left( \frac{\omega \rho t}{\sigma} \left( 1 + \left( 3^2 + \frac{\beta^2}{32} \right)^{\frac{1}{2}} + 0.85 \frac{d}{t} \right) \right) \quad (2)$$

where  $\omega$  is the angular frequency,  $c$  is the speed of sound,  $\eta$  is the viscosity,  $t$  is the thickness, and  $d$  is the hole diameter.  $\beta$  is a perforation constant dependent on the properties of the fluid and can be expressed as:

$$\beta = d \sqrt{\frac{\omega \rho}{4\eta}} \quad (3)$$

where  $\rho$  is the mass density of air.

MPP absorbers should be considered as a combination of the panel itself and the acoustic environment it is positioned in. Most research has assumed a constant-depth backing cavity behind the MPP, where the normal incident impedance can be expressed as:

$$z = z_{tr} - j\rho c \cot(kD) \quad (4)$$

where  $k$  is the wavenumber defined as  $k = \omega/c$ , and  $D$  is the depth of the backing cavity. The normal incident sound absorption can be expressed as:

$$a_n = \frac{4r_n}{(1+r_n)^2 + (x_n)^2} \quad (5)$$

where  $r_n$  and  $x_n$  are the normalized real and imaginary parts of the impedance respectively. Note that Equation 5 is only valid if plane-wave propagation is assumed behind the MPP. That implies

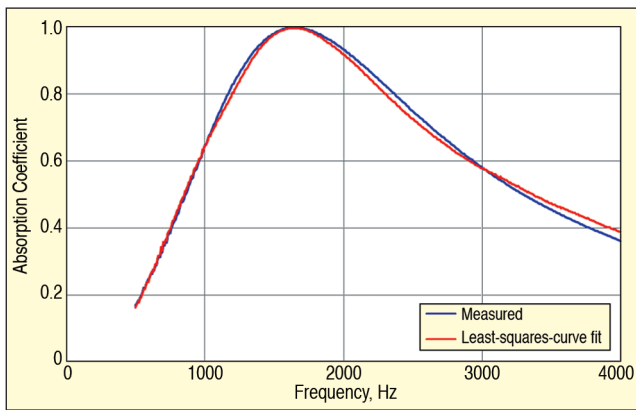


Figure 3. Comparison of measured and least-squares-curve-fitted sound absorption.<sup>7</sup>

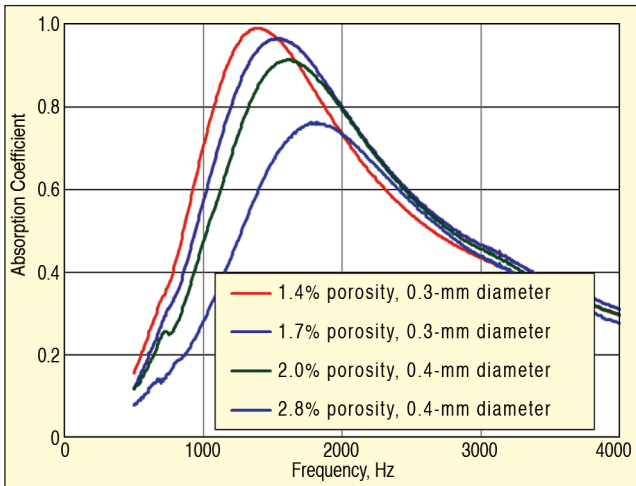


Figure 4. Sound absorption for different levels of dust accumulation.<sup>8</sup>

that the backing cavity will need to be broken up in some way for most applications. Otherwise, the sound absorption coefficient will likely be much lower than predicted in Equation 5.

Equation 2 assumes that perforations are circular and uniform in diameter. Other perforation geometries have been modeled using CFD,<sup>6</sup> and the use of CFD is recommended if designing new panels.

If a current product is being used, the sound absorption can be measured for an MPP with a known cavity depth, and effective parameters for the porosity and perforation diameter can be determined using a nonlinear least-squares curve fit.<sup>7</sup> Normally, an average thickness is assumed. Once the effective parameters are known, the transfer impedance can be predicted at lower or higher frequencies than those for which the impedance tube can normally be used. Such measurements aid in better understanding the effects of making adjustments to perforation rate or slit size and can be used to fine tune manufacturing processes. Figure 3 compares the fitted to the measured sound absorption. In this case, the perforation rate and perforation diameter are 4.1% and 0.24 mm respectively if a nominal thickness of 1 mm is used.

### Effect of Dust Accumulation and Contamination

Designers frequently raise concerns about using MPP absorbers in environments where the perforations are likely to be partially filled with dust or particulate contamination as in under hood applications or in mufflers or silencers. Nonetheless, MPP absorbers have been successfully used in these applications.

The impact of contamination was studied by applying charcoal and aluminum oxide powder to the surface of an MPP.<sup>7,8</sup> Particle sizes ranged from approximately 40 to 80 microns. An airbrush was used to spray the powder onto an MPP oriented in a direction normal to the flow. Flow speed was adjusted so that dust would accumulate but not dislodge. The absorption coefficient was measured in an impedance tube hung vertically so that the accumulated dust in the slit was undisturbed during the measurement.

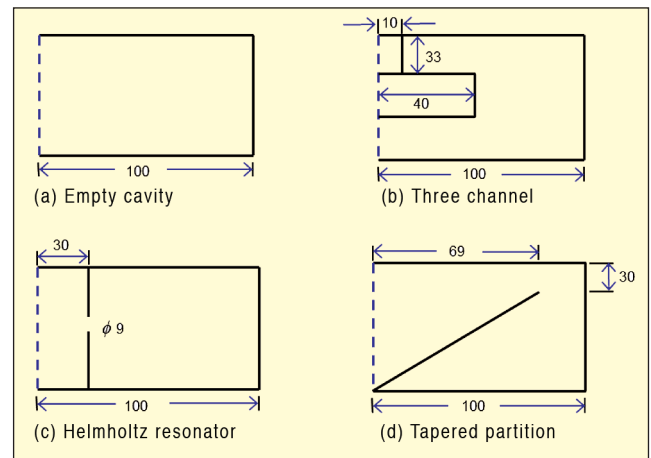


Figure 5. Schematics of backings for MPP: (a) empty cavity, (b) three-channel, (c) Helmholtz resonator, and (d) tapered partition; dimensions in mm.<sup>17</sup>

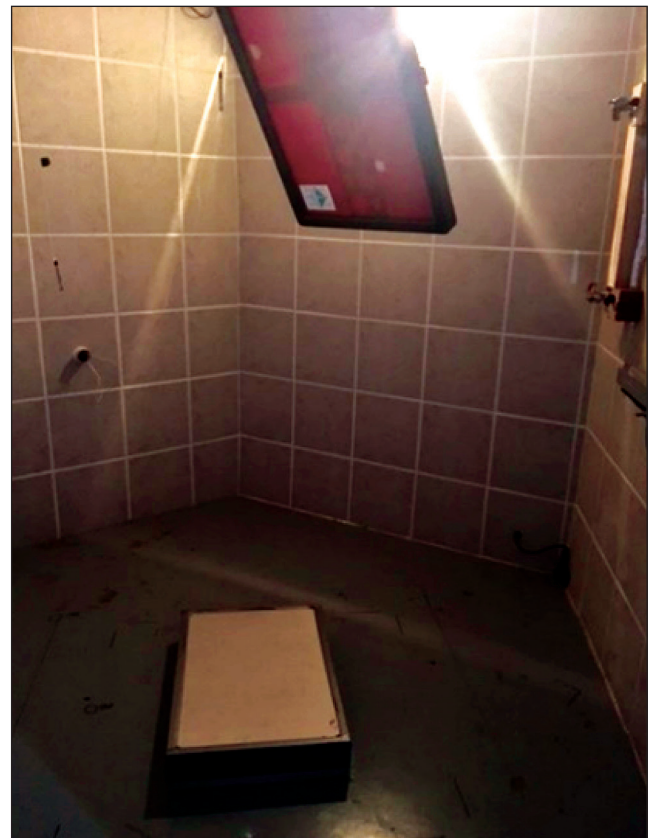


Figure 6. Sample on floor of small reverberation room.<sup>17</sup>

It seemed reasonable that dust accumulation would affect both the effective perforation rate and the perforation diameter. To test this conjecture, effective parameters were determined using the curve-fitting approach discussed earlier. As an example, a 0.3-mm-thick MPP was selected with circular perforations. Figure 4 shows the impact of contamination on the sound absorption. The effective porosity and hole diameter are included in the legend. It can be observed that the sound absorption coefficient is actually increased as the perforations become filled.

But note that the more fundamental conclusion is that the effective perforation rate decreases significantly as dust accumulates and that the perforation diameter only decreases slightly. This is an important observation for design purposes. In other cases, contamination may degrade the performance of the MPP, particularly if the panel is thicker.<sup>8</sup> Nevertheless, designers can estimate the potential impact of contamination by simply reducing the porosity in Maa's equation.

It also noteworthy that the MPP was heavily polluted with the pores barely visible for the most contaminated cases. Though dust



Figure 7. Partitioning behind MPP.

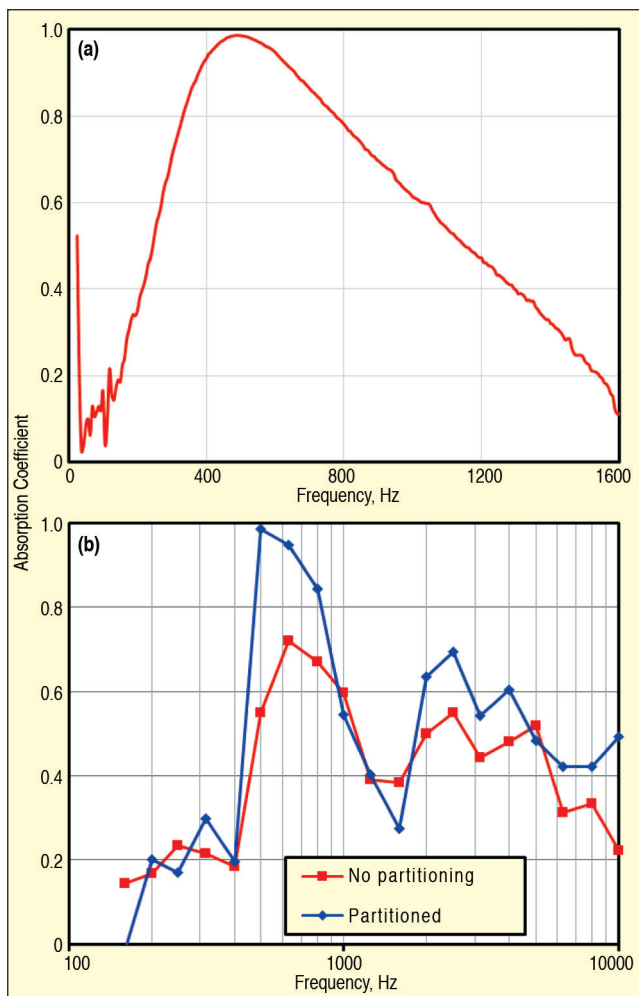


Figure 8. Sound absorption with empty cavity: (a) normal-incidence sound absorption; (b) diffuse-field sound absorption without and with partitioning.<sup>17</sup>

affects performance, the MPP nevertheless remains functional even when heavily contaminated. These results, as well as the aforementioned real-world applications, suggest that many of the concerns about dust contamination are unfounded. The results in Figure 4 would suggest that a thin MPP will perform better in a dusty environment.

### Adding Special Backings to Improve Performance

Not only was Maa's seminal paper published in 1975, but also a means to improve the performance by adding special backings was suggested by Wirt.<sup>9</sup> MPP absorbers are tunable. One way to do so is to vary the perforation rate or pore diameter. Sometimes a range of perforation sizes is introduced across a panel; this broadens



Figure 9. Three-channel backings installed behind MPP: (a) cells fully populated with backings; (b) alternating cells with backings.

the frequency range of effectiveness. However, the ability to tune the absorber by solely varying the perforations is limited. For best results, the depth of the backing cavity should be varied.

Recall that the MPP relies on viscous friction. The amount of energy dissipated is related to the particle velocity in the holes, and losses are greater when the velocity is high. Acoustic particle velocity is minimal next to a hard surface but will be high at approximately one-fourth acoustic wavelength from the hard surface. That is where the MPP should be placed to maximize the dissipation.

In the results shown earlier, the normal incident sound absorption was measured and examined. This should approximate the performance of the sound absorber if the direction of wave propagation is normal to the panel. In prior work,<sup>10-12</sup> it was demonstrated that the MPP absorber would behave like a locally reacting sound absorber if the backing cavity is partitioned. In particular, attenuation of grazing waves is significantly augmented. Similarly, Yu *et al.*<sup>13</sup> and Yang *et al.*<sup>14</sup> applied partitioning behind a MPP in ducts with predictably good results. Though partitioning may be accomplished in a number of ways, the most common practice has likely been to add honeycomb partitioning into the air space between the MPP and wall.<sup>15</sup>

Additional benefit has been observed if the cavity depth can be varied in the air space. These ideas are in no way new. In a brilliant paper from the 1970s,<sup>9</sup> Wirt, who was working for Lockheed, suggested configuring channels in a number of interesting arrangements behind a resistive screen. If the resistive screen is replaced by a MPP absorber, the absorbers that Wirt designed can be given new life.

Our research group<sup>16,17</sup> built on Wirt's ideas and demonstrated that broadband and low-frequency sound absorption could be enhanced by filling the space between an MPP and wall with a designed backing. Other researchers have tried similar strategies. Wang and Huang,<sup>18</sup> for instance, also varied the cavity depth be-

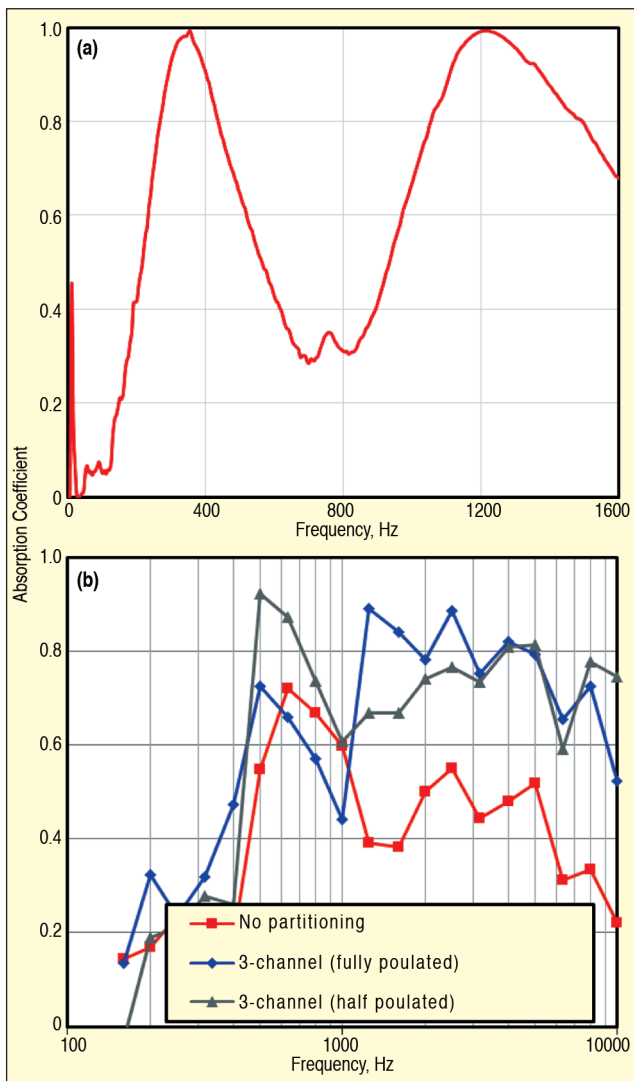


Figure 10. Sound absorption with three-channel backing: (a) normal-incidence sound absorption; (b) diffuse-field sound absorption with cells fully and half populated.<sup>17</sup>

hind the MPP. Park<sup>19</sup> placed a tuned Helmholtz resonator behind the MPP to target low-frequency noise. Zhao and Fan<sup>20</sup> placed mechanical impedance plates behind the MPP, which functions similarly to a Helmholtz resonator.

### Absorption Results for MPP with Designed Backings

Four different backing configurations are considered including;

- Empty airspace
- Three channel
- Helmholtz resonator
- Tapered partition

The configurations are illustrated in Figure 5. The normal-incidence sound absorption for each of the backings was measured using ASTM E1050<sup>2</sup> and the diffuse field incidence using a variation of ASTM C423.<sup>21,22</sup> The normal-incidence sound absorption was measured using a square cross-section impedance tube.

Though normal-incidence results are of interest, the diffuse-field sound absorption coefficient is perhaps more indicative of the performance of the MPP absorbers in an enclosure. Diffuse-field sound absorption measurements were performed in a 10.87 m<sup>3</sup> reverberation room with an approximately 2 m-high ceiling and no parallel walls. Based on past investigations, the reverberation room is suitable for tests above 150 Hz.<sup>21</sup>

The sound source is a distributed-field loudspeaker, and test samples were prepared and fitted into a 0.6 × 0.4 m metal box with wood frame on border. Figure 6 shows one of the samples positioned on the floor of the small reverberation room. The test temperature is approximately 20 °C and the humidity is ~58-62%.

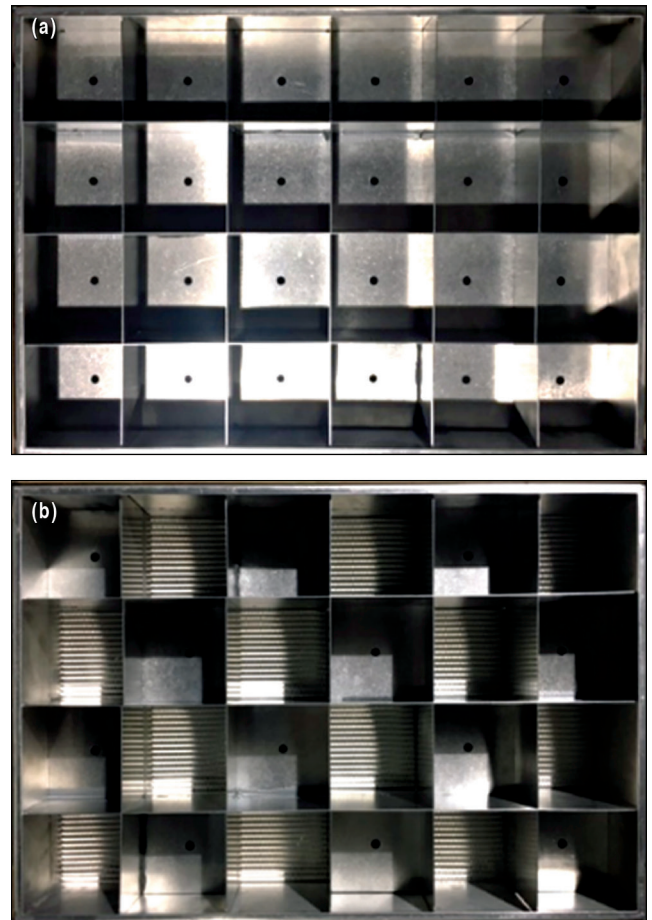


Figure 11. Helmholtz resonator backings installed behind MPP: (a) cells fully populated with backings; (b) alternating cells with backings.

The metal box contained 24 cells, each with a 0.1 m × 0.1-m size. This size is similar to the square impedance tube cross section. Samples were placed at the center of the reverberation room in the same position for all tests. Though neither the reverberation room nor sample size are as large as would be desired, the results should be usable on a comparative basis.

The baseline case is for the MPP with an empty cavity backing (Figure 5a). Aluminum partitioning is added behind the MPP, as shown in Figure 7. The normal incidence (ASTM E1050) and diffuse-field sound absorption (approximating ASTM C423) are shown in Figure 8a and 8b, respectively. Note that the frequency scales are different. Figure 8b illustrates the impact of adding partitioning to the airspace between the MPP and floor. It can be seen that the diffuse field sound absorption is improved at most frequencies and especially between 500 and 1000 Hz. Though the sound absorption is appreciable *sans* partitioning, it is evident that an additional 1-2 dB overall might be gained by partitioning; this could be critical depending on the application.

In an effort to improve the high-frequency sound absorption, three channels of varying depth are introduced in Figure 5b. It follows that the sound absorber should perform well in three different frequency bands with each cavity depth tuned to a different band. The lower channel wraps around the middle channel and terminates at the upper channel termination. So the lower channel is effectively longer than the spacing between the MPP and wall. This longer channel length is expected to improve the lower-frequency attenuation. Recently, Gai *et al.*<sup>23</sup> used a set of similar L-shaped cavities; this is functionally equivalent.

Two variations of the three-channel backing were considered. In the first, the three-channel backing is used in each partition (see Figure 9a). The second strategy is to alternate between the three-channel and empty cavity backings, as shown in Figure 9b. Sound absorption results are shown for normal and diffuse-field incidence in Figures 10a and 10b, respectively. Though improvement would be anticipated at the lower frequencies based on the

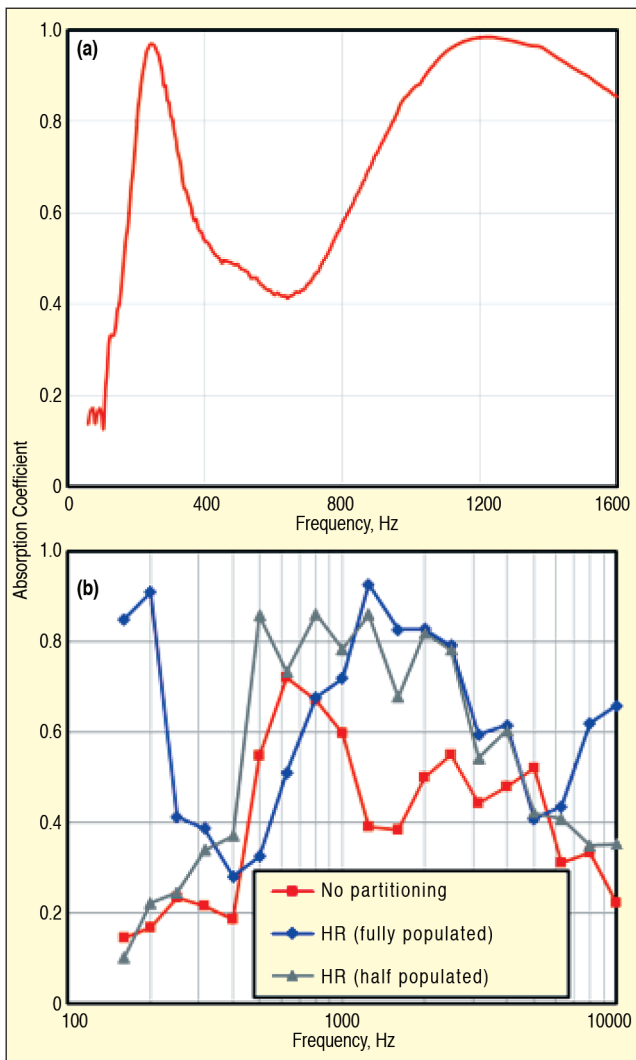


Figure 12. Sound absorption with Helmholtz resonator (HR) backing: (a) normal-incidence sound absorption; (b) diffuse-field sound absorption with cells fully and half populated.<sup>17</sup>

normal incident sound absorption, it can be seen that this does not translate to the diffuse-field sound absorption. Very little if any improvement is observed at low frequencies. Nevertheless, the performance is greatly improved above 1000 Hz. An improvement on the order of 2-3 dB might be anticipated in a product.

Another option considered was to introduce a Helmholtz resonator behind the MPP, as shown in Figure 5c. At low frequencies, the MPP is nearly acoustically transparent, since the particle velocity in the perforate will be relatively low. So it is anticipated that the Helmholtz resonator will dominate at low frequencies, while the MPP is expected to be effective at high frequencies with the shorter cavity depth. Figure 11 shows a photograph of the Helmholtz resonators inserted in each cell. Configurations are considered with the cells fully populated with Helmholtz resonators and with alternating empty cells and Helmholtz resonators.

Figure 12a shows the normal-incidence sound absorption. As anticipated, the Helmholtz resonator is very effective at ~300 Hz, while the MPP takes over above ~1000 Hz. Figure 12b shows the diffuse-field sound absorption. In the fully populated case, the Helmholtz resonators appear to be effective at low frequencies, though they are not for the half-populated case. It is possible that the measurement is inaccurate using the small reverberation room at low frequencies, so no concrete conclusion should be made. Nevertheless, the performance is greatly improved at high frequencies, and the half-populated case agreeably balances low- and high-frequency performance needs.

The tapered configuration in Figure 5d is functionally equivalent to the Helmholtz resonator of Figure 5c. The upper left-hand triangle functions as a variable-depth cavity providing broadband

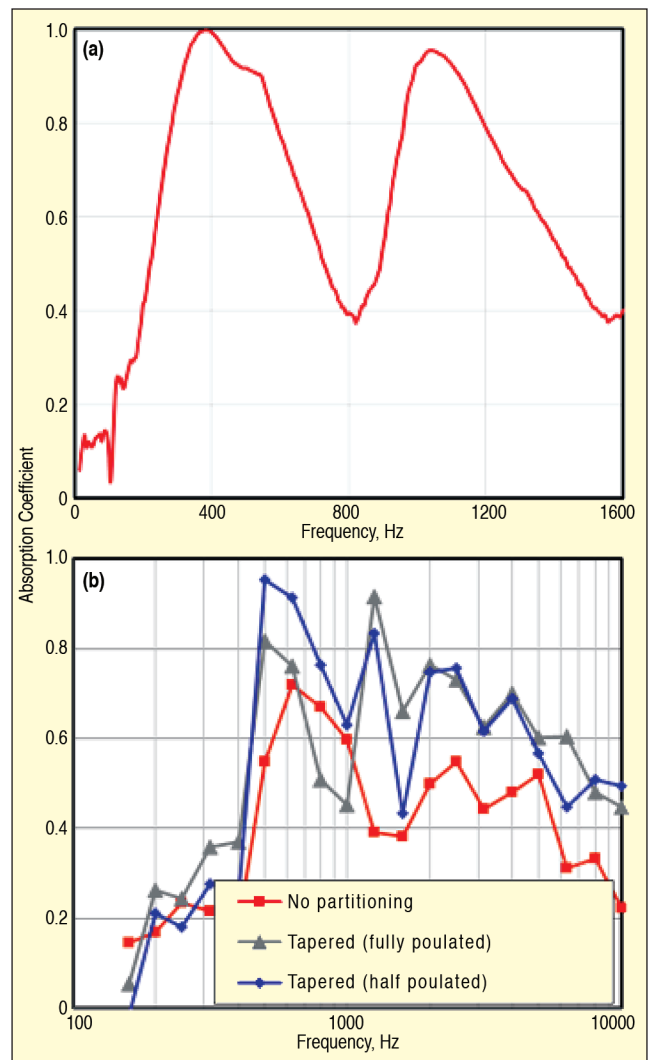


Figure 13. Sound absorption with tapered backing: (a) normal-incidence sound absorption; (b) diffuse-field sound absorption with cells fully and half populated.<sup>17</sup>

attenuation. The lower right triangle functions as a Helmholtz resonator whose neck is the opening connecting the upper and lower chambers. Figure 13a shows the normal-incidence sound absorption. Excellent performance between 300 and 600 Hz is observed. Moreover, appreciable broadband sound absorption can be seen. Figure 13b shows the diffuse-field sound absorption. Whether using a full- or half-populated strategy, the sound absorptive performance is improved throughout the frequency range. An improvement on the order of 2-3 dB might be anticipated in a product.

### Double-Leaf MPP Absorbers

Another popular approach has been to use multi-leaf configurations to improve performance. Sakagami *et al.*<sup>24,25</sup> and Zhang and Gu<sup>26</sup> used double-leaf MPP configurations to improve the broadband absorption. Sakagami *et al.*<sup>25</sup> inserted honeycomb partitioning between the two layers to force plane wave behavior in between the perforated layers; this proved advantageous. Figures 14a and 14b show a schematic and photograph, respectively, of a thin double-leaf MPP with honeycomb between the two MPP layers.

The double-leaf MPP normal-incidence and diffuse-field sound absorption are shown in Figures 15a and 15b, respectively. The normal-incidence sound absorption is slightly improved over the entire frequency. However, the diffuse-field sound absorption is greatly improved at frequencies above ~2000 Hz. There may be a functional advantage in using the double-leaf MPP in many applications because it is especially stiff.

### Summary

MPP absorbers are primarily used in applications where rugged-

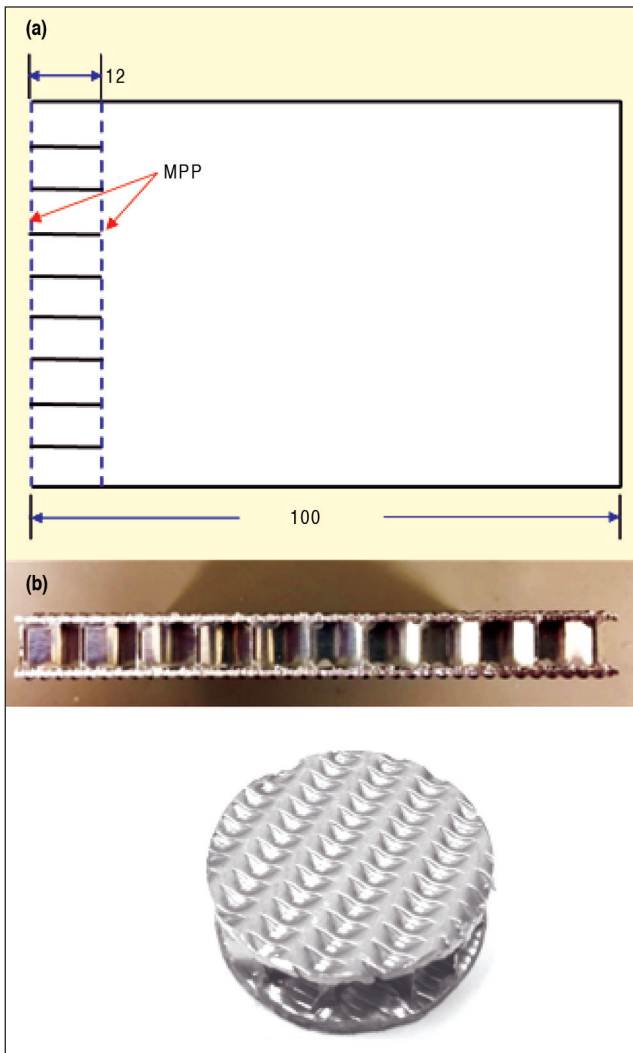


Figure 14. Double-leaf MPP with honeycomb partitioning between panels: a) schematic; (b) photographs.<sup>17</sup>

ness, cleanability, and aesthetics drive the design. They require considerable care when integrating them into a product to ensure good sound absorptive performance.

In this article, recommendations are provided for integrating MPP absorbers into a product. The MPP should first be characterized by measuring the transfer impedance and determining effective geometric parameters using a least-squares curve fit. These effective parameters can be used to adjust the transfer impedance in accordance with the environment in which the MPP is placed. These include temperature, grazing flow, and high sound pressure levels.

After selecting and characterizing the MPP, attention should then be shifted to the airspace behind the MPP. The performance can be improved significantly if the cavity is partitioned, and additional performance can be achieved by creatively varying the backing cavity depth.

Which backing design is better? That depends on the application and other considerations outside of the sound absorptive performance. The primary hurdles to widespread use are now manufacturability and cost. Can MPP and backing combinations be developed that are cost effective, durable, and in sufficient volume? Design, manufacturing, and noise and vibration engineers will need to work closely with one another on these problems.

### Acknowledgments

The authors gratefully acknowledge the support of the Vibro-Acoustics Consortium for this work.

### References

1. D. W. Herrin, J. Liu, and A. F. Seybert, "Properties and Applications of

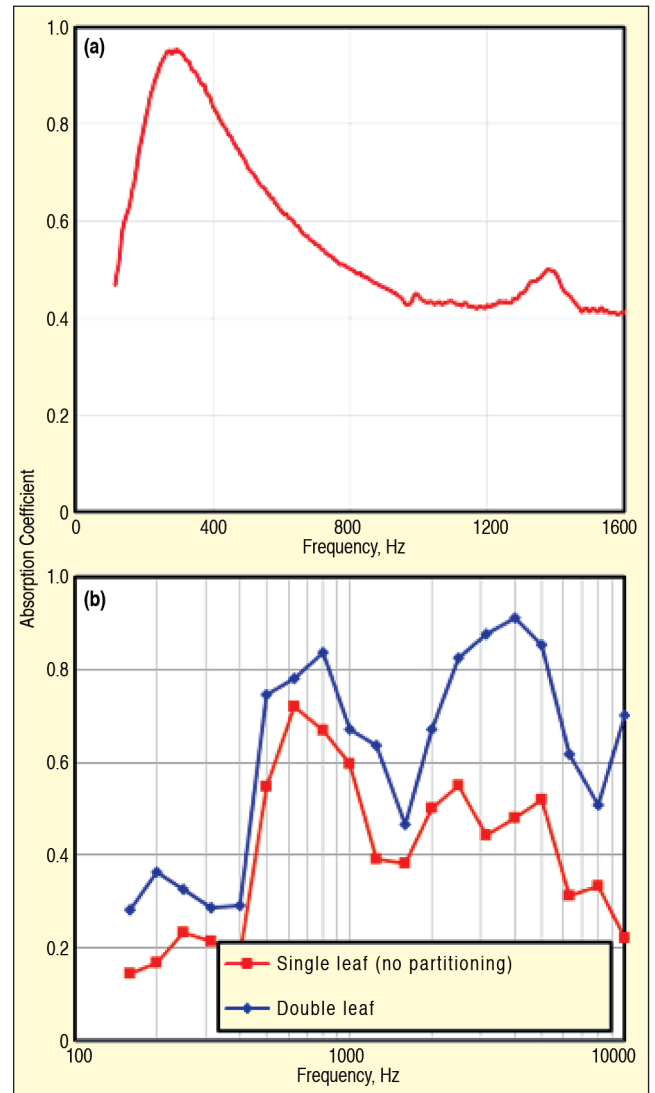


Figure 15. Sound absorption with double-leaf configuration: (a) normal-incidence sound absorption; (b) diffuse-field sound absorption compared to MPP without partitioning.<sup>17</sup>

2. "Microperforated Panels," *Sound & Vibration*, 2011.
3. ASTM E1050-98, Standard Test Method for Impedance and Absorption of Acoustical Materials using a Tube, Two Microphones and a Digital Frequency Analysis System, American Society of Testing and Materials, 1998.
4. ASTM C522-09, Standard Test Method for Airflow Resistance of Acoustical Materials, American Society for Testing and Materials, 2009.
5. D. A. Bies and C. H. Hansen, *Engineering Noise Control and Practice*, Fourth Edition, CRC Press, 2009.
6. D. Y. Maa, "Theory and Design of Microperforated-Panel Sound-Absorbing Construction," *Scientia Sinica XVIII*, pp. 55-71, 1975.
7. J. S. Bolton and N. Kim, *Use of CFD to Calculate the Dynamic Resistive End Correction for Microperforated Materials*, Acoustics Australia, Vol. 38, No. 3, 2010.
8. J. Liu, X. Hua, and D. W. Herrin, "Estimation of Effective Parameters for Microperforated Panel Absorbers and Applications," *Applied Acoustics*, Vol. 75, pp. 86-93, 2014.
9. J. Liu and D. W. Herrin, "Effect of Contamination on Acoustic Performance of Microperforated Panels," *SAE International Journal of Passenger Cars - Mechanical Systems*, Vol. 4, No. 2, pp. 1156-1161, 2011.
10. L. S. Wirt, "Sound-Absorptive Materials to Meet Special Requirements," *Journal of the Acoustical Society of America*, Vol. 57, No. 1, pp. 126-143, 1975.
11. J. Liu and D. W. Herrin, "Enhancing Micro-Perforated Panel Attenuation by Partitioning the Adjoining Cavity," *Applied Acoustics*, Vol. 71, pp. 120-127, 2010.
12. M. Yairi, K. Sakagami, M. Morimoto, and A. Minemura, "Acoustical Properties of Microperforated Panel Absorbers with Various Configurations of the Back Cavity," 12th International Congress on Sound and Vibration, Lisbon, Portugal, 2005.
13. M. Toyoda, and D. Takahashi, "Sound Transmission through a Microperforated Panel Structure with Subdivided Air Cavities," *Journal of the Acoustical Society of America*, Vol. 124, pp. 3594-3603, 2008.
14. X. Yu, L. Cheng, and X. You, "Hybrid silencers with micro-perforated

- panels and internal partitions," *Journal of the Acoustical Society of America*, Vol. 137, No. 2, pp. 951-962, 2015.
14. C. Yang, L. Cheng, and Z. Hu, "Reducing interior noise in a cylinder using micro-perforated panels," *Applied Acoustics*, Vol. 95, pp. 50-56, 2015.
  15. C. Yang and L. Cheng, "Sound absorption of microperforated panels inside compact acoustic enclosures," *Journal of Sound and Vibration*, Vol. 360, pp. 140-155, 2016.
  16. X. Hua, D. W. Herrin, and P. Jackson, "Enhancing the Performance of Microperforated Panel Absorbers by Designing Custom Backings," *SAE International Journal of Passenger Cars – Mechanical Systems*, Vol. 6, No. 2, 2013.
  17. W. Liu, D. W. Herrin, and E. Bianchini, "Diffuse Field Sound Absorption of Microperforated Panels with Special Backings," *SAE International Journal of Vehicle Dynamics, Stability and NVH*, Vol. 1, No. 2, 2017.
  18. C. Wang and L. Huang, "On the acoustic properties of parallel arrangement of multiple micro-perforated panel absorbers with different cavity depths," *Journal of the Acoustical Society of America*, Vol. 130, No. 1, pp. 208-218, 2011.
  19. S-H Park, "Acoustic Properties Of Micro-Perforated Panel Absorbers Backed by Helmholtz Resonators for the Improvement of Low-Frequency Sound Absorption," *Journal of Sound and Vibration*, Vol. 332, pp. 4895-4911, 2013.
  20. X. Zhao and X. Fan, "Enhancing Low-Frequency Sound Absorption of Micro-Perforated Panel Absorbers by Using Mechanical Impedance Plates," *Applied Acoustics*, Vol. 88, pp. 123-128.
  21. P. Jackson, "Design and Construction of a Small Reverberation Chamber," SAE Noise and Vibration Conference, Paper No. 2003-01-1679, Traverse City, MI, 2003.
  22. ASTM Standard C423, Standard test method for sound absorption and sound absorption coefficients by the reverberation room method, 2009.
  23. X. L. Gai, T. Xing, X. H. Li, B. Zhang, F. Wang, Z. N. Cai, and Y. Han, "Sound absorption of microperforated panel with L shape division cavity structure," *Applied Acoustics*, Vol. 122, pp.41-50, 2017.
  24. K. Sakagami, M. Morimoto and W. Koike, "A Numerical Study of Double-Leaf Microperforated Panel Absorbers," *Applied Acoustics*, Vol. 67, pp. 609-619, 2006.
  25. K. Sakagami, M. Yairi, and M. Morimoto, "Multiple-Leaf Sound Absorbers with Microperforated Panels: an Overview," *Acoustics Australia*, Vol. 38, No. 2, pp. 76-81, 2010.
  26. Z. M. Zhang and X. T. Gu, "The Theoretical and Application Study on a Double-Layer Microperforated Sound Absorption Structure," *Journal of Sound and Vibration*, Vol. 215, No. 3, pp. 399-405, 1998. 

The author can be reached at: [david.herrin@uky.edu](mailto:david.herrin@uky.edu).